

Hydrocalumite and Its Polymer Derivatives. 1. Reversible Thermal Behavior of Friedel's Salt: A Direct Observation by Means of High-Temperature in Situ Powder X-ray Diffraction

Laetitia Vieille, Isabelle Rousselot, Fabrice Leroux, Jean-Pierre Besse, and
Christine Taviot-Guého*

Laboratoire des Matériaux Inorganiques, UMR 6002, Université Blaise Pascal
(Clermont-Ferrand II), 24 avenue des Landais, 63177 Aubière Cedex, France

Received April 8, 2003. Revised Manuscript Received July 23, 2003

The structure of the phases obtained upon dehydration and decomposition of Friedel's salt $[\text{Ca}_2\text{Al}(\text{OH})_6]\text{Cl}\cdot 2\text{H}_2\text{O}$, also known as hydrocalumite, was investigated by several experimental techniques, in particular, high-temperature in situ XRD measurements, which allowed the detection of a metastable intermediate phase. Thermogravimetric analyses show that Friedel's salt, like most of the layered double hydroxides, undergoes a three-step decomposition on heating (dehydration, dehydroxylation, and anion expulsion) over the following temperature ranges: 25–280, 280–400, and >400 °C. Sharp phase transitions are observed as a result of the ordered distribution of Ca and Al atoms in the hydroxide layer and the well-ordered interlayer structure. Upon cooling to room temperature and exposure to the atmosphere, the dehydrated phase obtained by calcination between 80 and 280 °C was found to recover the basal spacing characteristic of hydrated galleries (7.81 Å) within a few minutes. The structural determination of this thermally metastable phase based on X-ray powder diffraction data recorded at 116 °C reveals a quasi-pillared layer structure with chloride anions situated midway in the interlamellar space at only 2.904(3) Å from Ca atoms of adjacent hydroxide layers. Friedel's salt becomes amorphous at ca. 400 °C, and above 750 °C, it crystallizes into a mixture of CaO and mayenite $\text{Ca}_{12}\text{Al}_{14}\text{O}_{33}$. Exposure of the amorphous residue obtained at 400 °C to aqueous solutions of KCl led to reconstruction–intercalation phenomena.

Introduction

Layered double hydroxides (LDH) are an important class of materials currently receiving considerable attention for a wide variety of applications in catalysis and environmental remediation.^{1–5} In particular, Friedel's salt $[\text{Ca}_2\text{Al}(\text{OH})_6]\text{Cl}\cdot 2\text{H}_2\text{O}$, also called hydrocalumite, and abbreviated hereafter as $\text{Ca}_2\text{Al}-\text{Cl}$ is structurally one of the best understood of the layered double hydroxides and can serve as a model for other less ordered LDH.^{6–8} These layered Ca-aluminate hydrates are also known collectively as AFm phases in the cement

science literature.⁹ The layered crystal structure of LDH is built by the periodical stacking of positively charged $(\text{M}^{2+}, \text{M}^{3+})(\text{OH})_6$ octahedral layers related to brucite $\text{Mg}(\text{OH})_2$ and negatively charged interlayers consisting of anions and water molecules. For AFm phases, Ca^{2+} and M^{3+} ions (Al^{3+} , Fe^{3+} , Ga^{3+} , and Sc^{3+}) are ordered in the hydroxide layers and the interlayer water molecules are coordinated to Ca atoms, creating 7-fold-coordinated Ca sites.

As precursors of mixed oxide catalysts, the thermal behavior of LDH has been extensively reviewed.^{10–13} The Mg–Al system is especially remarkable since the oxide residues undergo reconstruction, even on standing in air by the adsorption of CO_2 and H_2O from the atmosphere. This reversible thermal behavior exhibited only by a few LDH is exploited for the synthesis of novel

* To whom correspondence should be addressed. E-mail: gueho@chimsrv1.univ-bpclermont.fr.

(1) Trifiro, F.; Vaccari, V. In *Comprehensive Supramolecular Chemistry*; Atwood, J. L., Davies, J. E. D., MacNicol, D. D., Vogtle, F., Eds.; Pergamon: Oxford, 1996; Vol. 7, p 251.

(2) De Roy, A. *Mol. Cryst. Liq. Cryst.* **1998**, *311*, 173.

(3) Vaccari, A. *Appl. Clay. Sci.* **1999**, *14*, 161.

(4) Rives, V.; Ulibarri, M. A. *Coord. Chem. Rev.* **1999**, *181*, 61.

(5) (a) Inacio, J.; Taviot-Guého, C.; Forano, C.; Besse, J. P. *Appl. Clay Sci.* **2001**, *18*, 255. (b) Lopez-Salinas, E.; Llanos-Serrano, E.; Cortes-Jacome, A.; Schifter-Secora, I. *J. Porous Mater.* **1996**, *2*, 291–297.

(6) Allmann, R. N. *Jb. Miner. Mh.* **1977**, 136.

(7) (a) Terzis, A.; Philippakis, S.; Kuzel, H. J.; Burzlaff, H. Z. *Kristallogr.* **1987**, *181*, 29. (b) Renaudin, G.; Kubel, F.; Rivera, J. P.; François, M. *Cem. Concr. Res.* **1999**, *29*, 1937. (c) Rousselot, I.; Taviot-Guého, C.; Leroux, F.; Leone, P.; Palvadeau, P.; Besse, J. P. *J. Solid State Chem.* **2002**, *167*, 137.

(8) (a) Roussel, H.; Briois, V.; Elkaim, E.; de Roy, A.; Besse, J. P. *J. Phys. Chem.* **2000**, *B25*, 5915. (b) Roussel, H.; Briois, V.; Elkaim, E.; de Roy, A.; Besse, J. P.; Jolivet, J. P. *Chem. Mater.* **2001**, *13*, 329.

(9) Taylor, H. F. W. *Cement chemistry*, 2nd ed.; Thomas Telford Publishing: London, 1997.

(10) Puttaswamy, N. S.; Vishnu Kamath, P. *J. Mater. Chem.* **1997**, *7*, 1941.

(11) Kanazaki, E. *Inorg. Chem.* **1998**, *37*, 2588.

(12) (a) Stanimirova, TS.; Vergilov, I.; Kirov, G. *J. Mater. Sci.* **1999**, *34*, 4153. (b) Rives, V. *Inorg. Chem.* **1999**, *38*, 406. (c) Vaysse, C.; Guerlou-Demourgues, L.; Delmas, C. *Inorg. Chem.* **2002**, *41*, 6905.

(13) Aramendia, M. A.; Aviles, Y.; Borau, V.; Luque, J. M.; Marinas, J. M.; Ruiz, J. R.; Urbano, F. J. *J. Mater. Chem.* **1999**, *9*, 1603.

intercalates of LDH.^{14–18} Thermal decomposition of LDH is thus a highly significant process for both the synthesis of catalysts and the reconstruction–intercalation mechanism. Yet despite these numerous investigations, the process of thermal decomposition of LDHs is still a matter of debate.¹² For instance, in the Mg/Al/CO₃ system, there have been different opinions about the reconstruction mechanism, the duration, and mechanism of evolution of H₂O and CO₂. Of promising interest is the use of in situ techniques. Recently, by means of in situ high-temperature powder X-ray diffraction (HTXRD) measurements, Kanezaki¹¹ has detected a thermally metastable phase between 150 and 400 °C for a Mg/Al-layered double hydroxide. Such in situ measurements through which the temperature of the sample is kept constant allow a detailed examination of the change in the layered structure of LDH.

In the present study, we aim at clarifying the composition, structure, and properties of thermally decomposed phases of Friedel's salt, particularly in the temperature interval 20–300 °C to understand the processes of decomposition and regeneration of hydrocalumite-like materials. Structural changes in the layered structure of [Ca₂Al(OH)₆]Cl·2H₂O subjected to thermal treatment were monitored from in situ HTXRD, thermogravimetric analyses, and MAS NMR. The information gathered here enable a better understanding of the organic hydrocalumite derivatives presented in the companion paper.

Experimental Section

Sample Preparation and Chemical Analysis. Friedel's salt was prepared by the coprecipitation method at a controlled pH similar to that described by Miyata.¹⁹ The synthesis was carried out at 65 °C under vigorous magnetic stirring using deionized decarbonated water as well as a nitrogen atmosphere to prevent incorporation of atmospheric CO₂. Ten milliliters of a mixed solution of 0.66 M CaCl₂·2H₂O and 0.33 M AlCl₃·6H₂O was added dropwise to a reactor previously filled with 250 mL of a mixture consisting of water and ethanol in a 2:3 volumetric ratio. The pH was kept constant at 11.5 ± 0.1 by the simultaneous addition of 2.0 M NaOH. After complete addition of the metallic salts, the precipitate was aged in the mother solution for 24 h. The precipitate obtained was then centrifuged, washed twice with water by forming a slurry in water followed by centrifugation, and finally dried in a vacuum at room temperature.

Elemental analyses were performed at the Vernaison Analysis Center of CNRS. The composition was [Ca_{2.01}Al_{1.00}(OH)₆Cl_{1.00}·2H₂O]·0.29H₂O·0.31CO₂, which indicates that the amount of chloride exactly balances the positive charge of the main layers, thus excluding the presence of carbonate anions in the interlamellar space. Detected carbon is thus likely to be due to physisorbed CO₂, as often reported for LDH owing to their basic character.²⁰ The analyses also show the presence of physisorbed water.²¹

Reconstruction Procedure. The calcinations were conducted at four different temperatures based on XRD and TGA results, namely, 300, 350, 400, and 450 °C. Samples were heated in a tubular furnace for 12 h with a heating rate of 5 °C/min. About 50 mg of the resulting mixed oxides was then brought into 50 mL of deionized and decarbonated water and stirred for 24 h under a nitrogen atmosphere so as to ensure complete dispersion of the materials. To these suspensions 0.265 g of KCl was added and magnetic stirring was maintained overnight; the quantity of anions was about 20 times that necessary for stoichiometric anion exchange. The products were recovered by centrifuging and washing with water and then dried in a vacuum at room temperature.

In Situ X-ray Diffraction. Powder X-ray diffraction patterns were recorded on a X'Pert Pro Philips diffractometer, with Cu Kα radiation and a diffracted beam graphite monochromator. A high-temperature chamber (Anton Paar HTK-16) was installed, enabling in situ high-temperature measurements under a controlled atmosphere. Measurements were carried out in a static air atmosphere or under dynamic vacuum in the temperature range 25–1000 °C, after 30 min equilibration at each temperature, and the heating/cooling rate was 60 °C/min. Repetitive treatments consisting of calcinations at increased temperatures and subsequent cooling to room temperature were performed, leading to two different sets of data, those obtained in situ at high temperature and those recorded after the sample was cooled to room temperature. Typical measurement conditions were in the 2θ range 2–75°, step size 0.05° (2θ), and step counting time 20 s.

High-Temperature Structure Refinement. For the structural investigation of the dehydrated phase at 116 °C, the powder was deposited on a glass slide to eliminate platinum diffraction lines. The sample was held for 2 h at that temperature before the measurement was started. Data were recorded in the angular range 2–70° (2θ) in steps of 0.012° with a count time of 40 s at each point. The program FULLPROF²² was used for the Rietveld refinement. The intensities of the reflections were calculated using the analytical pseudo-Voigt peak-shape function; the background was defined by linear interpolation between points in the patterns. The weak peak at 29.29° (2θ) corresponds to the most intense line of the diffraction pattern of calcite CaCO₃. Owing to the very low intensity of this reflection and since no reflection is expected in this region for Friedel's salt, the refinement was made by considering an excluded region between 28.9 and 29.8° (2θ). The structure was solved in the R $\bar{3}$ space group starting from the atomic positions of the room-temperature structure reported elsewhere and crystallizing in the same space group.^{7c} The position of the chloride anions and the absence of water molecules were ascertained by difference Fourier calculations.²³ The final refinement of the atomic positions along with the isotropic atomic displacement factors, the scale factor, and the profile parameters led to acceptable R-factor values gathered in Table 1. The values of the isotropic atomic displacement factors are quite reasonable, in particular, for chloride anions, which may indicate an ordered distribution of these anions in agreement with their localization on symmetry centers.

Thermal Analysis. Thermogravimetric analyses were performed on a Setaram TGA 92 instrument. A complete thermogram was first recorded in the temperature range 25–1200 °C in a static air atmosphere with a heating rate of 5.0 °C/min to identify the different mass losses. The reversibility of the dehydration step was then investigated by recording the gain in mass on cooling after heating the sample at two different temperatures, 100 and 150 °C. To combine XRD and TGA results, the same heating program was used.

(14) Sato, T.; Kato, K.; Endo, T.; Shimada, M. *React. Solids* **1986**, *2*, 253.

(15) Kooli, F.; Depege, C.; Ennaqadi, A.; de Roy, A.; Besse, J. P. *Clays Clay Miner.* **1997**, *45*, 92.

(16) Rocha, J.; del Arco, M.; Rives, V.; Ulibarri, M. A. *J. Mater. Chem.* **1999**, *9*, 2499.

(17) Rajamathi, M.; Nataraja, G. D.; Ananthamurthy, S.; Kamath, P. V. *J. Mater. Chem.* **2000**, *10*, 2754.

(18) Hibino, J.; Tsunashima, A. *J. Mater. Sci. Lett.* **2000**, *19*, 1403.

(19) Miyata, S. *Clays Clay Miner.* **1983**, *31*, 305–311.

(20) Hibino, T.; Yamashita, Y.; Kosuge, K.; Tsunashima, A. *Clays Clay Miner.* **1995**, *4*, 427–432.

(21) Yun, S. K.; Pinnavia, T. *Chem. Mater.* **1995**, *7*, 348–354.

(22) Rodriguez-Carvajal, J. FULLPROF, A Program for Rietveld Refinement and Pattern Matching Analysis, *Abstracts of the Satellite Meeting on Powder Diffraction of the XV Congress of the IUCr*, Toulouse, France, 1990, p 127.

(23) Sheldrick, G. M. *SHELXL-97, Program for Crystal Structure Determination*; University of Cambridge: Cambridge, U.K., 1997.

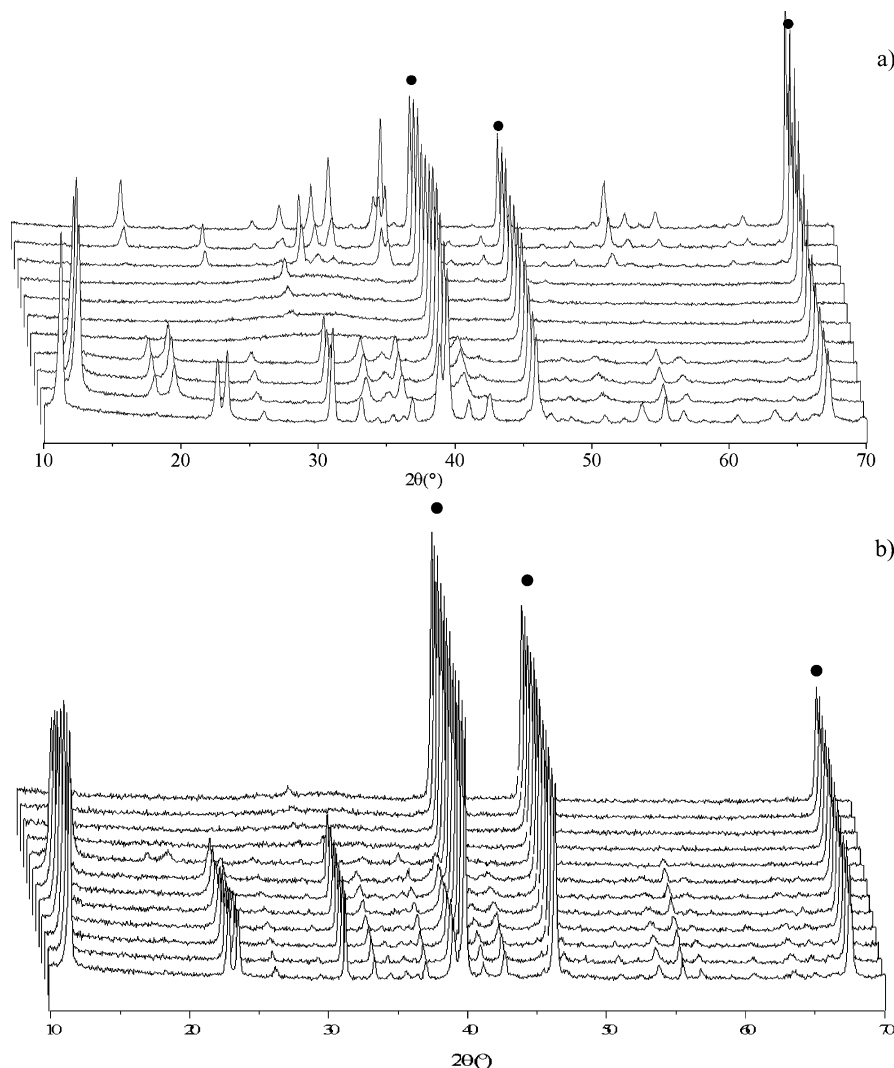


Figure 1. (a) High-temperature in situ powder diffraction patterns of $\text{Ca}_2\text{Al-Cl}$ under an ambient atmosphere at different temperatures ($^{\circ}\text{C}$) from bottom to top: 25, 100, 200, 280, 350, 450, 500, 650, 750, 850, and 950 (b) compared with those recorded after cooling to room temperature: 25, 80, 100, 120, 160, 200, 240, 280, 300, 350, 400, and 450 $^{\circ}\text{C}$.

Table 1. Rietveld Refinement Results of $\text{Ca}_2\text{Al}(\text{OH})_6\text{Cl}$ at 116 $^{\circ}\text{C}$

formula weight	244.61
space group	$R\bar{3}$
lattice parameters	
a (\AA)	5.7351(2)
c (\AA)	20.628(1)
volume (\AA^3)	587.57(4)
Z	3
temperature ($^{\circ}\text{C}$)	116
$\lambda_{\text{CuK}\alpha 1/\alpha 2}$ (\AA)	1.54056/1.54439
R_{wp} (%)	12.3/20.6(BC) ^a
χ^2	4.17

^a BC, background-corrected.

Ex Situ Characterization by IR and NMR Spectroscopies. The calcinations for ex situ experiments were performed in a tubular furnace in air for 12 h. Four temperatures were investigated, namely, room temperature, 100 $^{\circ}\text{C}$, 200 $^{\circ}\text{C}$, and 300 $^{\circ}\text{C}$ with a heating rate of 5 $^{\circ}\text{C}/\text{min}$. Fourier transform infrared (FTIR) spectra were recorded on a Perkin-Elmer 2000FT spectrometer using KBr pellets. ^{27}Al ($I = 5/2$) solid-state NMR experiments were performed on a Bruker 300 instrument at 78.20 MHz to investigate the Al coordination. The measurements were carried out using magic angle spinning (MAS) conditions at 10 kHz and a 4-mm-diameter rotor. $\text{Al}(\text{H}_2\text{O})_6^{3+}$ was used as a reference. Short radio frequency pulses associated with a recycling time of 500 ms were

used. Chemical shifts were not corrected from the second-order quadrupolar effect, which induces shift to lower frequency.²⁴

Results and Discussion

Figure 1 gives a general view of the X-ray diffraction patterns of $\text{Ca}_2\text{Al-Cl}$ in the whole temperature range recorded by means of in situ HTXRD under an ambient atmosphere. Repetitive treatments consisting of calcinations at increased temperatures and subsequent cooling to room temperature were performed. Two series of measurements are thus presented: those made in situ at high temperature (Figure 1a) and after the sample was cooled to room temperature (Figure 1b). Changes in the diffraction patterns indicate three steps in the thermal decomposition process over the temperature ranges $25 \leq T \leq 280$ $^{\circ}\text{C}$, $280 \leq T \leq 650$ $^{\circ}\text{C}$, and $650 \leq T \leq 950$ $^{\circ}\text{C}$, which are commonly ascribed to the following three main processes: dehydration, dehydroxylation, and anion decomposition. In the first temperature range, for room-temperature measurements, heating to 80 $^{\circ}\text{C}$ caused no significant change in the diffraction

(24) Engelhardt, G.; Michel, D. *High-Resolution Solid State NMR of Silicates and Zeolites*; Wiley: New York, 1987.

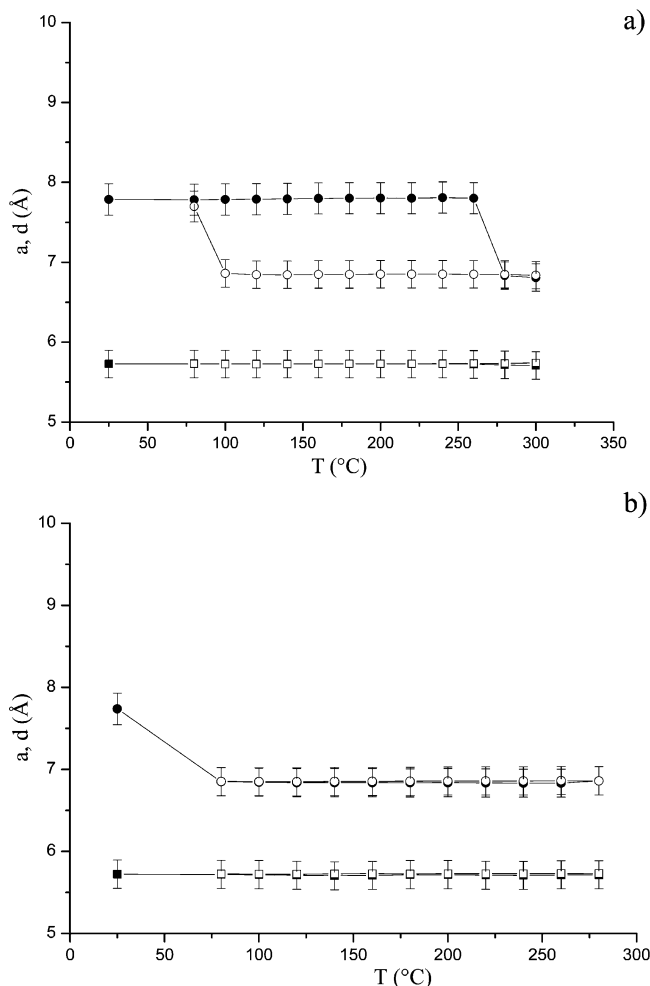


Figure 2. (a) Variation of a (square) and the basal spacing d_{003} (circle) for $\text{Ca}_2\text{Al-Cl}$ as a function of the temperature under an ambient atmosphere measured in situ (filled shapes) and after cooling to room temperature (open shapes) (b) compared with the values obtained under dynamic vacuum.

patterns, which agree well with published data for $\text{Ca}_2\text{-AlCl}$.^{7c} From the position of the strongest line of crystallographic indices (003), the interlayer spacing d_{003} was obtained. The lattice parameter a was estimated from the (110) diffraction at 31.2° (2θ) since $a = 2d_{110}$. Above 80 °C in situ measurements indicate a decrease of the basal spacing from 7.81 to 6.86 Å, while the in-plane dimension is not modified $a = 5.73$ Å (Figure 1a). These evolutions as a function of the temperature for both series of measurements are depicted in Figure 2a. Samples heat-treated up to 280 °C were found to rapidly recover their original structure on cooling upon exposure to the atmosphere, and since the layered structure is maintained, one can say that this reversible contraction is due to the reversible elimination of interlayer water molecules. At ca. 120 °C, the dehydrated phase goes through its maximum of crystallinity, as judged from the intensity of the reflections. Above this temperature, the reflections are broadened and reduced in intensity, perhaps due to concomitant partial dehydroxylation of the layers. Above 260 °C, both the hydrated and dehydrated phases are present on cooling and reversibility is completely lost at 280 °C. In the second temperature range, at 400 °C, dehydrated Friedel's salt is converted to an amorphous phase with very broad and indistinct XRD peaks. A calcination temperature of ca.

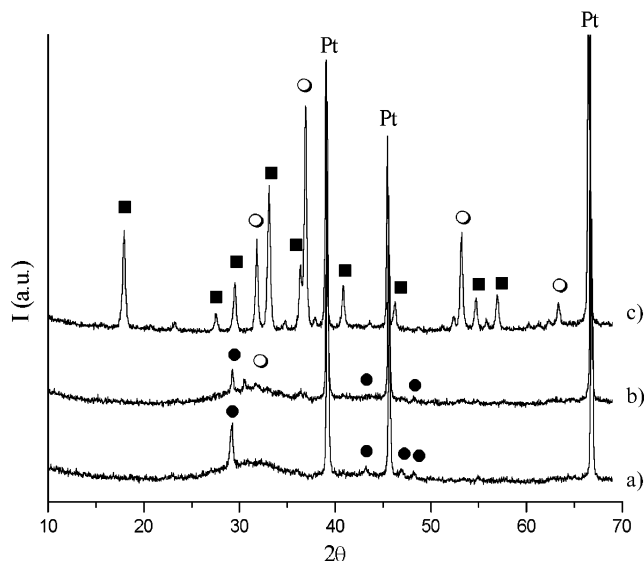


Figure 3. Room-temperature powder X-ray diffraction patterns of $\text{Ca}_2\text{Al-Cl}$ heat-treated at 600 °C (a), 700 °C (b), and 950 °C (c): ●, CaCO_3 ; ○, CaO ; ■, $\text{Ca}_{12}\text{Al}_{14}\text{O}_{33}$.

500 °C leads to the formation of crystalline calcite CaCO_3 , which starts transforming to CaO above 700 °C (Figure 3). Finally, raising the temperature up to 950 °C results in the formation of mayenite $\text{Ca}_{12}\text{Al}_{14}\text{O}_{33}$ and sharpening of CaO reflections.

To further confirm the involvement of water molecules from air in this reversible contraction, similar measurements were performed under dynamic vacuum (Figure 2b). As expected, the contraction observed for heat-treated samples is maintained at room temperature.

The water desorption behavior of Friedel's salt was also examined by thermogravimetric analysis. The TGA curve (Figure 4a) reveals three main weight losses over the temperature ranges $25 \leq T \leq 250$ °C, $250 \leq T \leq 400$ °C, and $400 \leq T \leq 1200$ °C, agreeing with XRD results. It is noticeable that the ordered structure of Friedel's salt yields a well-resolved TGA curve, suggesting sharp structural phase transitions upon heating. Consistent with the above interpretations, the mass loss of two water molecules computed according to the formula (12.8%) matches well the observed first mass loss (12.7%). The second loss (16.4%) is less than what is expected for the dehydroxylation of the hydroxide layers (19.2%). The third final weight loss (4.8%) of lesser significance than the previous two involves the sustained release of water molecules from the recombination of hydroxyl groups and anion decomposition. The slope at 1200 °C indicates that decomposition is not complete and may require prolonged standing at this temperature to be complete, as pointed out elsewhere.²⁵

To obtain quantitative estimates of the reversibility of the hydration–dehydration process, mass gain curves on cooling were recorded after heating the sample at 100 and 150 °C (Figure 4b). Sample heat-treated at 100 °C was found to regain up to 80% of its initial mass on cooling within 25 min only. This rate of rehydration or the kinetics of the rehydration reaction rapidly decreases with calcinations at higher temperature, and at 150 °C, only 50% mass gain is observed on cooling.

(25) Renaudin, G.; Rapin, J. P.; Humbert, B.; François, M. *Cem. Concr. Res.* **2000**, *30*, 307–314.

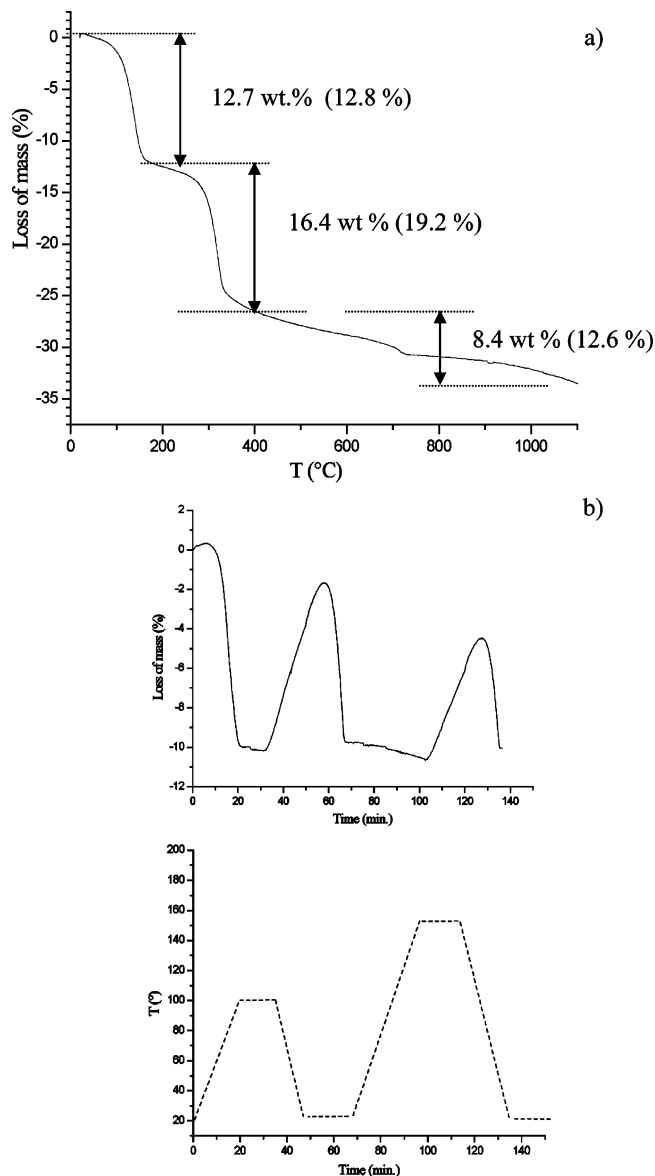


Figure 4. (a) Complete thermogram of $\text{Ca}_2\text{Al-Cl}$. (b) Mass gain curves on cooling after heating at 100 and 150 °C (mass gain curve on the top and heating program on the bottom).

Although the rehydration rate depends on the humidity level and other experimental conditions, this result

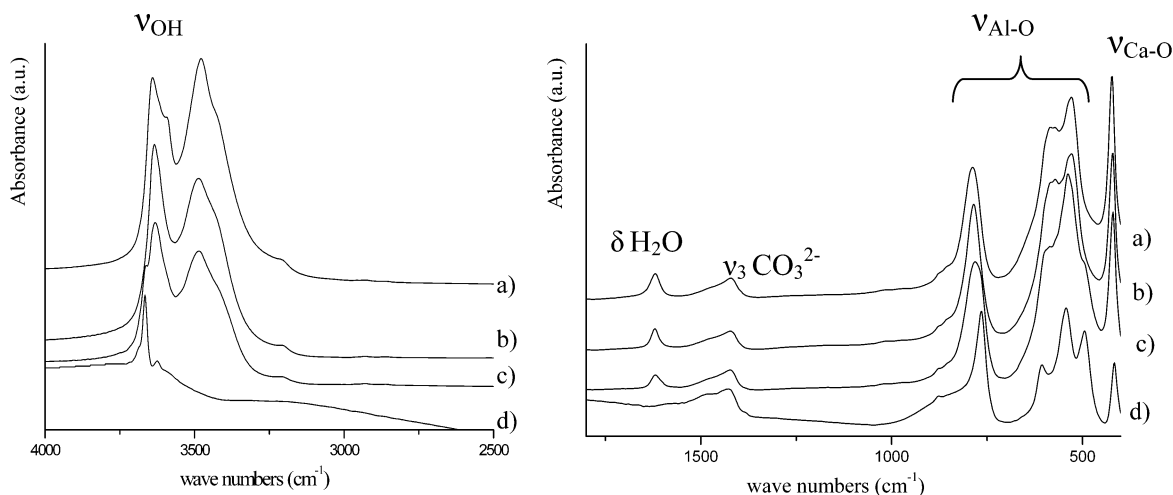


Figure 5. IR spectra of $\text{Ca}_2\text{Al-Cl}$ heat-treated at 100 °C (b), 200 °C (c), and 300 °C (d) compared with that of the as-prepared sample (a).

unequivocally evidences the reversibility of the dehydration process.

IR spectra of the samples heated in the temperature range 25–300 °C are also indicative of the transformation taking place upon heating, though they were not recorded in situ. Figure 5 shows those spectra measured at room temperature after the samples were heated at 100, 200, and 300 °C. The definitive removal of these water molecules between 200 and 300 °C is confirmed by the disappearance of the band at 1620 cm^{-1} assigned to an H_2O bending vibration. The disappearance of the broad absorption centered at 3480 cm^{-1} clearly indicates the major contribution of water molecules to this band. The gradual shift of the adjoining band from 3642 to 3666 cm^{-1} may be attributed to an increase in the force constant of the OH bond as a result of the vanishing of hydrogen bonding with interlayer water. Besides, the net decrease of the intensity of this band above 200 °C might indicate a partial dehydroxylation. Significant changes are also visible in the low-wavenumber region, characteristic of the lattice vibrations (shift of the absorption band from 788 to 766 cm^{-1}), pointing out the progressive collapse of the double-layered structure. On the other hand, under the thermal treatment conditions used, that is, calcinations in air, one would expect physisorbed CO_2 to be present on the outer surface of the crystallites.²⁰ This contamination occurs and is reflected by the relative broad and weak band at 1400 cm^{-1} typical of O–C–O vibrations (ν_3) for adsorbed (noninterlayer) carbonate anions. Finally, the appearance of shoulders at 1492 cm^{-1} (ν_3) and 879 cm^{-1} (ν_2) for the sample heated at 300 °C is in good agreement with the formation of calcite²⁶ as shown by X-ray diffraction.

To further examine the structural changes introduced by the release of interlayer water molecules in Friedel's salt, we followed the modifications in the Al^{3+} coordination by means of ^{27}Al solid-state MAS NMR. Like for IR analysis, NMR experiments were conducted ex situ. Displayed in Figure 6, the spectrum for the uncalcined phase contains a single resonance peak at ca. 8.5 ppm, consistent with an octahedral coordination of aluminum. Upon calcination in the temperature range 100–250 °C, this peak slightly shifts toward low-field values, indicating small changes around Al nuclei. Above 275 °C, the

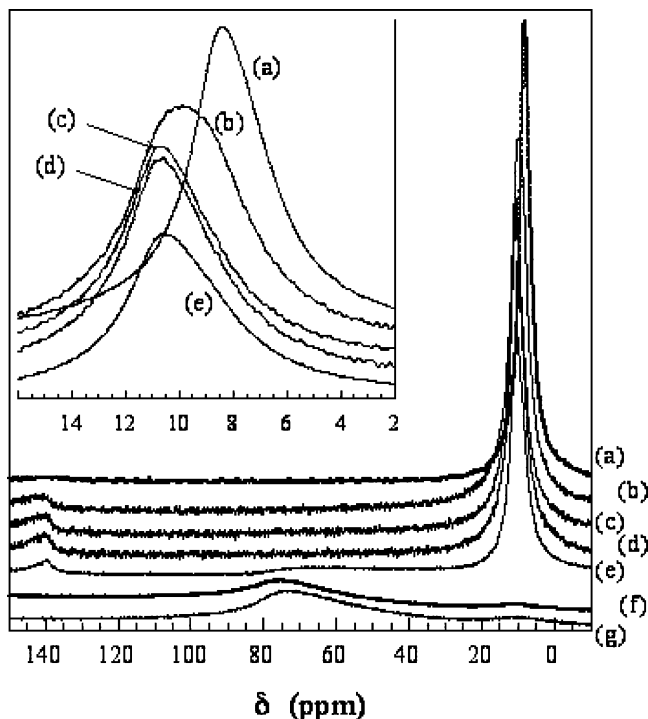


Figure 6. ^{27}Al solid-state NMR spectra of $\text{Ca}_2\text{Al-Cl}$ heat-treated at 100 °C (b), 200 °C (c), 250 °C (d), 275 °C (e), 300 °C (f), and (350 °C) compared with that of the as-prepared sample (a).

Table 2. Positional Parameters of $\text{Ca}_2\text{Al}(\text{OH})_6\text{Cl}$ at 116 °C

atom	site	x	y	z	B_{iso} (\AA^2)
Ca	6c	$2/3$	$1/3$	-0.0261(1)	1.95(9)
Al	3a	0	0	0	1.6(2)
OH	18f	0.3120(6)	0.0736(9)	0.0493(2)	4.9(2)
Cl	3b	0	0	$1/2$	9.8(2)

irreversible loss of interlayer water and a partial dehydroxylation of the layers result in the strong decrease of this resonance and the growth of a small resonance at $\delta \approx 75$ ppm that can be assigned to tetrahedrally coordinated aluminum; this latter resonance becomes more prominent upon calcination at higher temperature. In contrast to hydrotalcite related samples,¹⁶ the conversion of Al^{VI} to Al^{IV} is complete here and proceeds in a narrow temperature domain, that is, 275–300 °C. Exchange of chloride anions by organics will fade this collective process, different Al coordination sites being present simultaneously (see companion paper).

To construct an adequate structural model of the metastable dehydrated phase, we performed a structural study by Rietveld refinement of the in situ X-ray diffraction diagram recorded at 116 °C. Structural parameters are given in Table 2, and selected bond distances and angles are listed in Table 3. The observed, calculated, and difference profiles are displayed in Figure 7.

On prolonged heating from room temperature to 116 °C, the two structural water molecules are released from Friedel's salt as observed by TGA. This gives rise to a contraction of the interlamellar, which brings the chloride anions closer to the calcium atoms. The Ca–

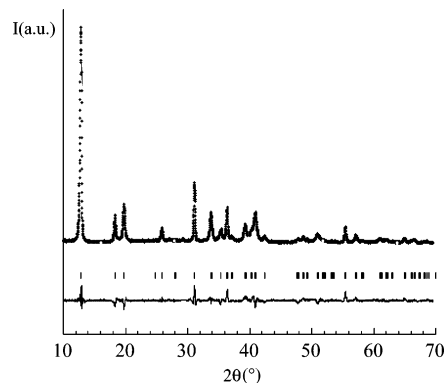


Figure 7. Experimental X-ray diffraction pattern (cross), calculated (line), Bragg reflections (ticks), and difference profiles for $\text{Ca}_2\text{Al-Cl}$ at 116 °C.

Table 3. Bond Lengths (\AA) and Angles ($^\circ$) in $\text{Ca}_2\text{Al}(\text{OH})_6\text{Cl}$ at 116 °C

Al ³⁺ –OH ($\times 6$)	1.913(4)
Ca–OH ($\times 3$)	2.396(5)
($\times 3$)	2.445(5)
Ca–Cl ($\times 2$)	2.900(3)
Cl–OH ($\times 6$)	3.407(4)
Al ³⁺ –Cl	4.7732(1)
layer thickness	2.03
interlayer thickness	4.84
OH–Al ³⁺ –OH	85.6(3)
	94.4(3)
	180.0(4)
OH–Ca–OH	65.0(2)
	82.5(2)
	88.0(2)
	108.1(2)
	147.0(3)
OH–Ca–Cl	78.7(2)
	130.4(2)
	81.8(1)

Cl distance obtained, that is, 2.900(3) \AA , is slightly longer than those found in calcium chloride hydrates generally ranging from 2.73 to 2.88 \AA .²⁷ Located midway in the interlayer space on a straight line passing through the Ca atoms, the chloride anions can thus nearly be considered as the seventh apex of Ca polyhedra, shared between two facing Ca polyhedra. In these conditions, an adjacent layer would be bridged by chloride anions as illustrated in Figure 8. Initially shifted by +0.59 \AA out of the center of its (OH)₆ octahedron in the fully hydrated phase,^{7c} the Ca atoms are shifted down from the (a,b) plane –0.54 \AA in the opposite direction to the chloride anions. Besides, the Ca–OH distances show an elongation of Ca(OH)₆ octahedra in the (a,b) plane (2.396 \AA) while distances along the c-axis slightly decrease (2.445 \AA); distances of 2.355 and 2.455 \AA respectively were found in the hydrated state. The Al–OH distances also decrease upon heating (1.913 \AA instead of 1.929 \AA), which may explain the slight shift observed by NMR. The overall effect of thermal dehydration on these octahedral layers is thus a small decrease of the a parameter while the layer thickness is not modified.

The Ca–Cl distance observed is to be intended as a lower limit value allowing rehydration. Above 280 °C, either chloride anions form a too close contact with calcium atoms or concomitant partial dehydroxylation

(26) Nakamoto, K. In *Infrared and Raman spectra of inorganic and coordination compound*, 4th ed.; Wiley: New York, 1986.

(27) Thewalt, U.; Bugg, C. *Acta Crystallogr.* **1973**, B29, 615–617.

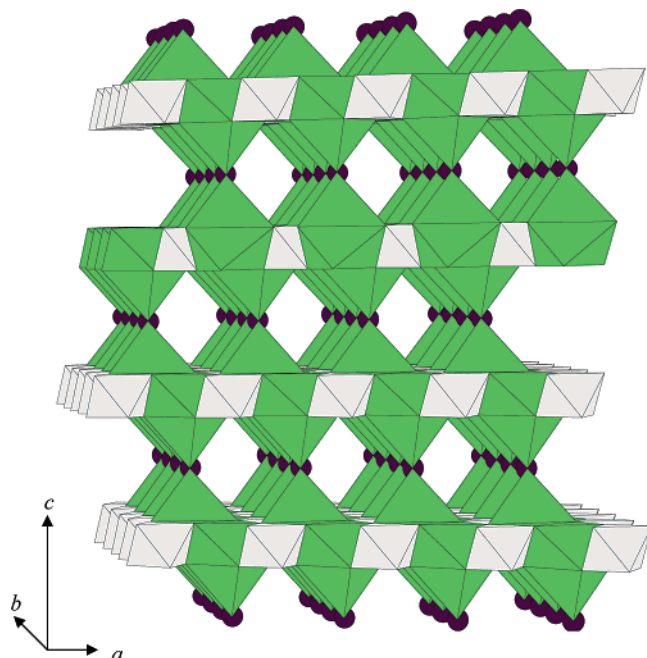


Figure 8. Crystal structure of dehydrated Friedel's salt at 116 °C. The main layers are drawn showing $\text{Al}(\text{OH})_6$ and $\text{Ca}(\text{OH})_6\text{Cl}$ polyhedra; in this representation, the main layers are bridged by chloride anions, forming a "pillar" structure.

occurs, both impeding the rehydration process. Such a "grafting" phenomenon at low temperature has already been mentioned for the nitrated AFm phase $\text{Ca}_2\text{Al}(\text{OH})_6\text{NO}_3 \cdot 4\text{H}_2\text{O}$ for which, around 70 °C, the main layers are bridged by nitrate groups, forming a pillar structure.²⁵ Another peculiarity of the nitrate phase, exhibited as well by the carbonate phases but not with halogenous anions, is the partial replacement at room temperature of the water molecules linked to Ca atoms by carbonate or nitrate anions.^{28,29}

Numerous studies on the thermal behavior of LDH have mentioned that the loss of structural water can be reversed upon exposure to the atmosphere but only a few have investigated the structural changes occurring during the dehydration process. Recently, by means of in situ HTXRD measurements, Kanazaki¹¹ has studied the reversible thermal behavior of MgAlCO_3 dehydrated phases obtained between 180 and 380 °C. These phases are metastable at room temperature and return quickly to the hydrated state in a wet atmosphere. According to the author, in this temperature range, the interlayer carbonates would react with interlayer water molecules, producing hydroxyl anions at the interlayer gallery which being unstable at room temperature cause the rapid reconstruction of the original structure. Other studies¹² have interpreted differently the thermal evolution of LDHS intercalated with carbonate anions from room temperature up to 300 °C. It would proceed in two steps with consecutive formation of two metaphases: one resulting from interlayer dehydration which, in contact with the atmosphere, reversibly transforms into the pristine phase; the second is formed at temperatures of 200–260 °C as a result of the dehydroxylation of a part

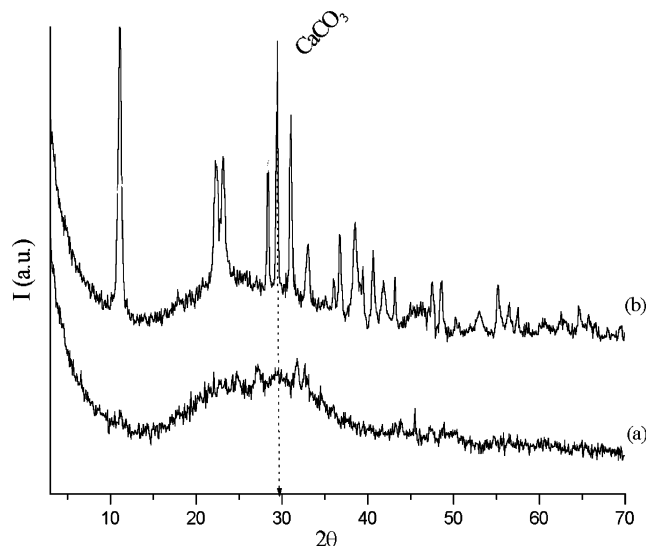


Figure 9. Powder X-ray diffraction patterns of $\text{Ca}_2\text{Al-Cl}$ heat-treated at 300 °C (a) compared with that obtained after a reconstruction–intercalation procedure in the presence of KCl (b).

of OH groups of the brucite-like layer and simultaneous inclusion of oxygen atoms from the CO_3^{2-} groups. Though sporadic, these different results might indicate that the structural changes in this low-temperature interval strongly depend on the whole composition of LDH.

An important feature of LDH is their ability to recover their original structure by exposure to an aqueous solution, provided that the original LDH contain volatile interlayer anions, leading to new compounds possessing novel physical and chemical properties. It has been proposed that the oxide residue obtained at this temperature with an amorphous X-ray diffraction pattern recalling the one of a rock salt structure is unstable and rapidly reconstructs to the parent hydroxide.¹⁷ Even though largely used for the incorporation of bulky guest molecules such as polyoxometalate anions into hydroxide related samples,^{30,31} the reconstruction process has not been established for hydrocalumite so far. In the present study, the temperature for which the layer structure collapses to an amorphous phase and reconstructs satisfactorily was found to be 400 °C (Figure 9). The reconstruction was carried out at ambient temperature in the presence of KCl solution. The X-ray diagram is in agreement with that of Friedel's salt, yet the large background hump observed may indicate that amorphous phases are present, which do not reconstruct once some Al has been extracted from the structure upon heating as shown by NMR.

Conclusion

Our results throw light on the changes which occur in Friedel's salt upon heating in air. Of particular interest here is the use of in situ techniques as most of the studies published are carried out at room temperature, where the state of the sample may have changed

(28) Renaudin, G.; François, M. *Acta Crystallogr.* **1999**, *C55*, 835–838.

(29) Renaudin, G.; François, M.; Evrard, O. *Cem. Concr. Res.* **1999**, *29*, 63–69.

(30) Chibwe, K.; Jones, W. *J. Chem. Soc., Chem. Commun.* **1989**, 926.

(31) Narita, E.; Kavizatna, P.; Pinnavaia, T. *J. Chem. Lett.* **1991**, 805.

during cooling, exposure to the atmosphere, or handling. In situ HTXRD measurements combined with thermogravimetric analysis show that the thermal decomposition of Friedel's salt, like most LDH, proceeds in three steps: quantitative dehydration between 80 and 280 °C followed by dehydroxylation between 280–450 °C, which overlaps to some extent with the anion decomposition. Sharp phase transitions are observed as a result of the ordered distribution of Ca and Al atoms in the hydroxide layer and the well-ordered interlayer structure. Friedel's salt becomes amorphous at ca. 400 °C, and above 750 °C, it crystallizes into a mixture of CaO and mayenite $\text{Ca}_{12}\text{Al}_{14}\text{O}_{33}$. Upon cooling to room temperature and exposure to the atmosphere, the dehydrated phase ($d_{003} = 6.86 \text{ \AA}$) was found to recover the basal spacing characteristic of hydrated galleries ($d_{003} = 7.81 \text{ \AA}$) within a few minutes only. Yet mass gain curves indicate that only the samples heating below 120 °C regain their original mass on cooling. Of course, this rehydration rate strongly depends on the experimental conditions and further measurements are needed to determine the controlling factors. The structural determination of this thermally metastable phase based on X-ray powder diffraction data recorded at 116 °C reveals a "quasi-pillared" layer structure with chloride anions situated midway in the interlamellar space at only

2.904(3) Å from Ca atoms of adjacent hydroxide layers. This Ca–Cl distance, slightly longer than those reported in calcium chloride, is to be intended as a lower limit value allowing rehydration. Above 280 °C, either chloride anions are irreversibly linked to calcium atoms or concomitant partial dehydroxylation occurs, both impeding the rehydration process. Such a "grafting" phenomenon at low temperature has also been reported for LDH with intercalated oxygen-containing anions but is scarcely known for non-oxygen-containing anions such as chloride anions.

The reconstruction phenomena demonstrated here for phases calcined at 400 °C is also quite remarkable since it has never been established for AFm materials so far. Like LDH, the residue prior to the reconstruction was found to be X-ray amorphous. A mechanistic study of this reversible thermal behavior is underway. Whether it proceeds via a dissolution–reconstruction process or involves a defect rock salt as mentioned for LDH or just a mixture of the unary oxides are points of interest.

Acknowledgment. The authors would like to thank Joël Cellier for his help in acquiring the in situ HTXRD data.

CM031069J